Interchain-Frustration-Induced Metallic State in Quasi-One-Dimensional Mott Insulators

M. Tsuchiizu,[1] Y. Suzumura,[1] and C. Bourbonnais[2]

[1]*Department of Physics, Nagoya University, Nagoya 464-8602, Japan*

[2]*Département de Physique, Université de Sherbrooke, Sherbrooke, Québec J1K-2R1, Canada*

(Received 28 January 2007; published 19 September 2007)

The mechanism that drives a metal-insulator transition in an undoped quasi-one-dimensional Mott insulator is examined in the framework of the Hubbard model with two different hoppings $t_{\perp 1}$ and $t_{\perp 2}$ between nearest-neighbor chains. By applying an $N_\perp$-chain renormalization group method at the two-loop level, we show how a metallic state emerges when both $t_{\perp 1}$ and $t_{\perp 2}$ exceed critical values. In the metallic phase, the quasiparticle weight becomes finite and develops a strong momentum dependence. We discuss the temperature dependence of the resistivity and the impact of our theory in the understanding of recent experiments on half-filled molecular conductors.

DOI: 10.1103/PhysRevLett.99.126404 PACS numbers: 71.10.Fd, 71.10.Pm, 71.30.+h

The remarkable properties of strongly correlated systems near a metal to Mott insulator (MI) transition stand out as one of the richest parts of the physics of strongly correlated systems [1]. This takes on particular importance in low dimensional materials at half-filling, and especially in one dimension, where spin and charge excitations are well-known to be invariably decoupled, an effect that receives experimental confirmation in the one-dimensional (1D) oxide material $SrCuO_2$ [2]. How this picture modifies when the hopping of electrons in more than one spatial direction progressively grows and a higher dimensional metallic ground state becomes possible is a key issue that remains poorly understood. This problem finds concrete applications in organic molecular compounds, which constitute very close realizations of 1D systems. This is the case notably of (TTM-TTP)I_3 and (DMTSA)BF_4 which, as genuine half-filled band materials due to the monovalent anions I_3^- and BF_4^-, see their Mott insulating state being gradually suppressed under pressure [3,4]. Quite recently, resistivity measurements on (TTM-TTP)I_3 at high pressure revealed that the temperature scale for the Mott insulating behavior is suppressed by an order of magnitude down to $T_{\mathrm{MI}} \approx 20$ K at $P = 8$ GPa of pressure, with a metallic ground state expected to occur above 10 GPa [5]. It is the objective of this Letter to propose a theoretical description of this transition.

Bosonization, renormalization group (RG) approaches to the 1D Hubbard model in weak coupling and its exact solution from the Bethe ansatz [6–8], show that electron-electron umklapp-scattering processes are a key ingredient that promotes the existence of a Mott insulating ground state at half-filling. The difficulty underlying the mechanism of the MI transition in the quasi-1D case resides in the fact that the decoupling of spin and charge excitations on the metallic side of the transition at higher dimension does not occur, namely, when Fermi-liquid quasiparticles excitations appear. This issue has been addressed theoretically by an RPA treatment of interchain hopping [9], in which its feedback effect on the Mott gap is neglected for the self-energy of the one-particle Green's function. The RPA results shows the existence of a Fermi-liquid metallic state with electron and hole Fermi-surface pockets when the interchain hopping exceeds a critical value. The important role of this feedback effect has been pointed out recently from the use of dynamical mean-field theory, extended to include the influence of 1D fluctuations (the chain-DMFT) [10]—an approach expected to be workable in the strong-coupling regime. In the weak-coupling regime, however, the electron-electron umklapp scattering and the characteristics of its coupling to nesting of the whole Fermi surface, play a key role [6–8], both for the Mott insulating state and for the possibility of the MI transition that emerges in the quasi-1D case. Transverse dispersion which has a tendency toward the realization of the deconfined metallic states [7,8,10] is in general overlooked in the calculation of one-particle Green's function from mean-field-like approaches. The two-loop RG approach avoids such an approximation and treats the Fermi-surface nesting conditions properly. These can be strongly altered in the quasi-1D case, especially in the presence of frustration in the electron kinetics.

In this Letter, we apply an $N_\perp$-chain RG approach to quasi-1D half-filled system as developed recently at the two-loop level [11,12]. The momentum dependence for nesting of the whole Fermi surface and that for couplings, including umklapp scattering [13–15], are taken into account in a systematic way in the calculation of one-particle Green's function and four-point vertices [11]. The combined impact of correlations and nesting frustration induced by interchain hopping on the transverse momentum dependence of the quasiparticle weight is obtained in weak-coupling regime.

We consider the quasi-1D half-filled Hubbard model on an anisotropic triangular lattice [Fig. 1(a)], with the transfer energies $t_\parallel \gg |t_{\perp 1}|, |t_{\perp 2}|$ ($t_\parallel$ is the energy along chains and $t_{\perp 1}$ and $t_{\perp 2}$ are those between chains). Our Hamiltonian, with the on site Coulomb repulsion U is given by

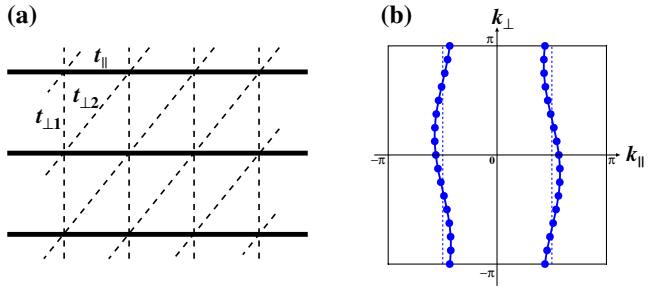

FIG. 1 (color online). (a) Lattice geometry of the present model. (b) The corresponding Fermi surface where the case for $N_\perp = 16$ is shown.

$$
\begin{aligned}
H = & -t_\parallel \sum_{j,\ell,s} (c^\dagger_{j,\ell,s} c_{j+1,\ell,s} + \text{H.c.}) \\
& - t_{\perp 1} \sum_{j,\ell,s} (c^\dagger_{j,\ell,s} c_{j,\ell+1,s} + \text{H.c.}) \\
& - t_{\perp 2} \sum_{j,\ell,s} (c^\dagger_{j,\ell,s} c_{j+1,\ell+1,s} + \text{H.c.}) \\
& + U \sum_{j,\ell} n_{j,\ell,\uparrow} n_{j,\ell,\downarrow} - \mu \sum_{j,\ell,s} c^\dagger_{j,\ell,s} c_{j,\ell,s}. \qquad (1)
\end{aligned}
$$

The operator $c_{j,\ell,s}$ denotes the annihilation of an electron on the jth site in the ℓth chain with spin s, and $n_{j,\ell,s} = c^\dagger_{j,\ell,s} c_{j,\ell,s} - \frac{1}{2}$. Here $\ell = 1, \ldots, N_\perp$ is the chain index. We take the continuum limit along the chain direction, whereas in the transverse direction we consider a finite system having an even number of chains $N_\perp$ with the boundary condition $c_{j,N_\perp+1,s} = c_{j,1,s}$. By applying a Fourier transform, the kinetic term can be rewritten as $H_0 = \sum_{\boldsymbol{k},s} \varepsilon(\boldsymbol{k}) c^\dagger_s(\boldsymbol{k}) c_s(\boldsymbol{k})$, where $\boldsymbol{k} \equiv (k_\parallel, k_\perp)$ and the energy dispersion is given by $\varepsilon(\boldsymbol{k}) = -2t_\parallel \cos k_\parallel - 2t_{\perp 1} \cos k_\perp - 2t_{\perp 2} \cos(k_\parallel + k_\perp) - \mu$. For $|t_{\perp i}| \ll t_\parallel$, the right- and left-moving electrons in the 1D case are well-defined due to an open Fermi surface [Fig. 1(b)] and the shape of the Fermi surface can be parametrized by the transverse momentum $k_\perp$ [11]. To lowest order in the interchain hoppings $t_{\perp 1}$ and $t_{\perp 2}$, the Fermi surfaces for right (+) and left (−) moving electrons, as a function of $k_\perp$, are given by $k^\pm_F(k_\perp) = \pm(\pi/2) \pm (t_{\perp 1}/t_\parallel) \cos k_\perp - (t_{\perp 2}/t_\parallel) \sin k_\perp$ and the chemical potential is $\mu = O(t^2_{\perp i})$. By considering the weak-interacting case and neglecting the $k_\perp$ dependence of the velocity, the linearized dispersion used in the RG method takes the simple form: $\varepsilon_p(\boldsymbol{k}) = pv[k_\parallel - k^p_F(k_\perp)]$ with $v = 2t_\parallel$ and $p = \pm$.

We follow the formulation of the two-loop RG method of Ref. [11] and first introduce the g-ology coupling constants [see Eq. (2.8) in Ref. [11]]:, namely, the backward ($g_{1\perp}$), forward ($g_{2\perp}$), and umklapp ($g_{3\perp}$) scatterings with opposite spins, and the forward scattering ($g_\parallel$) and umklapp ($g_{3\parallel}$) scatterings for parallel spins. The coupling constants are renormalized differently, developing an external—transverse—momenta dependence in the vertex corresponding to a patch-index dependence; that is, $g_\nu \to g_{\nu(q_\perp, k_{\perp 1}, k_{\perp 2})}$, where $k_{\perp 1}$ and $k_{\perp 2}$ are the transverse momenta for the right-going fermions, and $q_\perp$ is the momentum transfer [11]. The magnitude of the initial couplings are given by $g_{1\perp} = g_{2\perp} = g_{3\perp} = U$ and $g_\parallel = g_{3\parallel} = 0$. The RG equations are derived by scaling the bandwidth cutoff $\Lambda (\simeq 2\pi t_\parallel)$ as $\Lambda_l = \Lambda e^{-l}$, where l is the scaling parameter [11]. The explicit forms of the two-loop RG equations for all coupling constants in the case $t_{\perp 2} = 0$ are given in Ref. [11]. We solve here these two-loop RG equations numerically for a system with $N_\perp = 16$. For even $N_\perp$, the solution of the RG flows indicates the existence of a finite spin gap in the low-energy limit, which is expected to vanish in the infinite $N_\perp$ limit. The characteristic scale $l_{N_\perp}$ above which finite size effect would appear can be roughly estimated to be $l_{N_\perp} \approx \ln[\Lambda/|t_{\perp i} \sin(2\pi/N_\perp)|]$. For $N_\perp = 16$ and $t_{\perp 1}/t_\parallel = 0.1$ this gives $l_{N_\perp} \approx 5$, which is sufficient to obtain the MI transition without finite size effects for the present choice of parameters $U/t_\parallel = 2$ or 1.5.

For the bipartite lattice ($t_{\perp 2} = 0$), the system remains always insulating even for large $t_{\perp 1}$ [11]. This is due to perfect nesting condition for the Fermi surface. In this case the interchain hopping $t_{\perp 1}$ is relevant and becomes large under scaling procedure, and some umklapp couplings become small. However, a macroscopic number of these couplings remains relevant due to perfect nesting at vector $\boldsymbol{Q} = (\pi, \pi)$. In the case of large $t_{\perp 2}$, these relevant umklapp couplings are strongly reduced and all umklapp terms remain weak. The charge gap then collapses and a metallic state with a Fermi surface emerges as a consequence of nesting deviations that are introduced by large interchain frustration.

One-particle properties are best studied from the quasiparticle weight $z_{k_\perp}$. In the RG method at the two-loop level [11], the $k_\perp$ dependence of the self-energy is taken into account in a non perturbative way. This contrasts with the chain-DMFT, which treats the one-particle self-energy as a one-chain $k_\perp$-independent quantity of the one-particle Green's function [10]. In the RG formalism the transverse momentum dependence [11] is taken into account explicitly, and the quasiparticle weight of the one-particle Green's function takes the form $z_{k_\perp} \equiv z^n_{k_\perp} z^u_{k_\perp}$, where $z^n_{k_\perp}$ and $z^u_{k_\perp}$ are the contributions coming from the normal and umklapp parts of the scattering, respectively. Here, one can focus on the umklapp contribution $z^u_{k_\perp}$, since $z^n_{k_\perp}$ remains finite for $l < l_{N_\perp}$ in the metallic state. The explicit form of $z^u_{k_\perp}$ reads [11]

$$
z^u_{k_\perp} = \exp\left[-\frac{1}{2N^2_\perp} \sum_{q_\perp, k'_\perp} \int dl G^2_{\Sigma u(q_\perp, k_\perp, k'_\perp)} J^u_{1(q_\perp, k_\perp, k'_\perp)} \right], \qquad (2)
$$

$$
\begin{aligned}
G^2_{\Sigma u(q_\perp, k_\perp, k'_\perp)} \equiv & \; G^2_{c(q_\perp, k_\perp, k'_\perp)} + G^2_{c(\pi - q_\perp + k_\perp + k'_\perp, k_\perp, k'_\perp)} \\
& - G_{c(q_\perp, k_\perp, k'_\perp)} G_{c(\pi - q_\perp + k_\perp + k'_\perp, k_\perp, k'_\perp)}, \qquad (3)
\end{aligned}
$$

where $G_{c(q_\perp,k_\perp,k'_\perp)} \equiv g_{3\perp(q_\perp,k_\perp,\pi-k'_\perp)}/(2\pi v)$. The quantity $J^u_{1(q_\perp,k_\perp,k'_\perp)}$ is a cutoff function depending on the transverse dispersion [11] given by $J^u_{1(q_\perp,k_\perp,k'_\perp)} = 1$ for $|A'_{q_\perp,k_\perp,k'_\perp}| \ll \Lambda$ and $J^u_{1(q_\perp,k_\perp,k'_\perp)} \approx 0$ for $|A'_{q_\perp,k_\perp,k'_\perp}| \gg \Lambda$ where $A'_{q_\perp,k_\perp,k'_\perp} \equiv 2t_{\perp 1}[\cos k_\perp + \cos(k_\perp - q_\perp) - \cos k'_\perp - \cos(k'_\perp - q_\perp)] - 2t_{\perp 2}[\sin k_\perp - \sin(k_\perp - q_\perp) + \sin k'_\perp - \sin(k'_\perp - q_\perp)]$. The $k_\perp$ dependence of the umklapp-scattering contribution to $z_{k_\perp}$ for several values of $t_{\perp 2}$ at fixed $t_{\perp 1}/t_\parallel = 0.1$ is shown in Fig. 2(a). For weak frustration $t_{\perp 2}(<t^c_{\perp 2})$, this quantity is small showing the existence of an insulating phase with no low-energy quasiparticles. On the other hand, for strong frustration $t_{\perp 2}(>t^c_{\perp 2})$, it takes sizable values and shows a strong $k_\perp$ dependence. In the proximity of the insulating phase, the quantity $z^u_{k_\perp}$ presents a broad maximum around $k_\perp \approx \pm\pi/2$, which behavior implies the emergence of sections of Fermi surface [9], or "cold" regions around $\boldsymbol{k} \approx (k^p_F(\pm\pi/2), \pm\pi/2)$ [13]. The dips or "hot spots" in the quasiparticle weight correspond to regions of the Fermi surface where the nesting, within $2\pi/N_\perp$ accuracy, remain the most favorable. In the perfectly nested case no Fermi surface is found for any value of U. The overall profile is then intrinsically linked to the momentum dependent nesting properties over the whole Fermi surface [15]. These are not taken into account in previous analyses [9,10], which reach different conclusions in the weak-coupling regime.

The boundary for the metal-insulator transition can be determined analytically by noting that the metallic phase of the RG analysis is linked to the irrelevance of umklapp scattering. The metallic phase boundary can thus be obtained when the energy scale of imperfect nesting for umklapp scatterings becomes comparable to the energy scale Δ^{1D}_ρ [$\propto \sqrt{t_\parallel U}\exp(-2\pi t/U)$] of the 1D Mott gap. By noting that the nesting vector of the particle-hole loop, which couples to umklapp, is given by $\boldsymbol{Q} = (\pi, \pi \pm 2\alpha)$ with $\tan\alpha = t_{\perp 2}/t_{\perp 1}$, the degree of the imperfect nesting (the amplitude of the quantity $A'_{\pi\pm 2\alpha,k_\perp,k'_\perp}$) becomes $\sqrt{t^2_{\perp 1} + t^2_{\perp 2}}\sin 2\alpha$. The phase boundary for the MI transition is then determined by the condition

$$\frac{t_{\perp 1} t_{\perp 2}}{\sqrt{t^2_{\perp 1} + t^2_{\perp 2}}} = c\Delta^{1D}_\rho, \tag{4}$$

where c is a numerical constant being of the order of unity. The small difference between the numerical results and the above analytical expression comes from the renormalization of interchain hopping due to the normal scattering processes. The Mott gap is also renormalized by interchain hopping. The ground-state phase diagram in the $(t_{\perp 1}/t_\parallel, t_{\perp 2}/t_\parallel)$ plane is shown in Fig. 2(b), where the dotted line denotes Eq. (4). The ambiguities in the cutoff functions of the RG [11,14] prevent us from obtaining a precise location of the phase boundary.

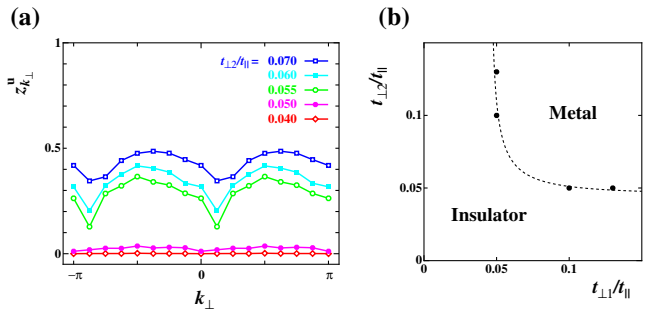

FIG. 2 (color online). (a) Umklapp-scattering contribution of the quasiparticle weight $z^u_{k_\perp}$ for $U/t_\parallel = 2$ and $t_{\perp 1}/t_\parallel = 0.1$, with several $t_{\perp 2}$. (b) Ground-state phase diagram on the plane of $t_{\perp 1}/t_\parallel$ and $t_{\perp 2}/t_\parallel$. The dotted line denotes the condition of Eq. (4).

The Mott transition has also been addressed in two-dimensional Hubbard model on an anisotropic triangular lattice with nearest-neighbor hopping t and next-nearest-neighbor hopping t' [16]. The present model (1) can be connected to the two-dimensional Hubbard model by taking $t_\parallel \to t$, $t_{\perp 1} \to t$, and $t_{\perp 2} \to t'$. While our approach is restricted to the small interchain hopping, the metal-insulator transition obtained here for finite frustration is consistent with the numerical results in two dimensions.

From the solution of the scaling flows of the umklapp scatterings, the temperature dependence of the resistivity can be qualitatively calculated from the memory function approach combined with the RG method by using $l = \ln(\Lambda/T)$ [8,17]. By extending the approach to the quasi-1D case, the perturbative expression of the conductivity reads $\rho(T) \propto N_\perp^{-3}\sum_{q_\perp,k_\perp,k'_\perp} G^2_{c(q_\perp,k_\perp,k'_\perp)}(l)e^{-l}$. While this formula is not valid for large $t_{\perp i}/T$ [17], it will depict the qualitative temperature dependence of resistivity. Typical behaviors of the resistivity for $\Delta^{1D}_\rho < t_{\perp 1}$, obtained from this formula, are shown in Fig. 3(a). At high temperature ($T > t_{\perp 1}$, $t_{\perp 2}$), the effects of interchain kinetics are masked due to the thermal fluctuations where the Tomonaga-Luttinger (TL) liquid behavior is reproduced. At low temperature, the insulating behavior can be seen for small $t_{\perp 2}$, while the metallic behavior is found for strong frustration (large $t_{\perp 2}$). A finite-temperature phase diagram, as a function of $t_{\perp 2}$, can be obtained from this behavior, as shown schematically in Fig. 3(b). At high temperature, the TL liquid state is realized, which is followed in the crossover region by the development of a Fermi surface. The effect of the frustration is yet masked by thermal fluctuations; i.e., this region can be described effectively by a nested Fermi surface. At further low temperature, the state moves to the Mott insulator or the Fermi-liquid (FL) state depending on $t_{\perp 2}$. In the FL state, the effect of $t_{\perp 2}$ becomes prominent and the nesting conditions of the full Fermi surface are altered. It can also be seen from Fig. 3(a) that the characteristic temperature $T_{\rm FL}$ at which the crossover to the metallic FL state takes place increases with $t_{\perp 2}$. For $\Delta^{1D}_\rho > t_{\perp 1}$, on the other hand, a direct crossover from the TL liquid state to the Mott insulator would be seen, and

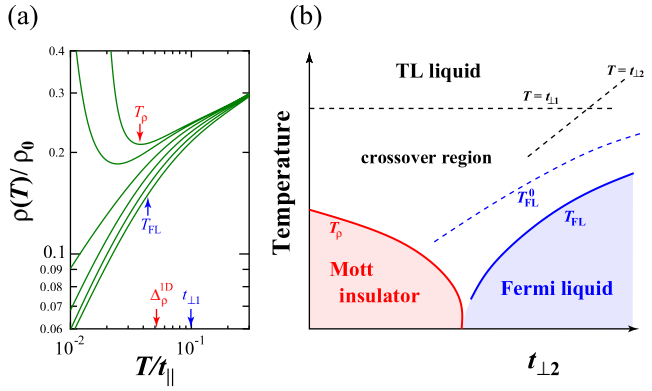

FIG. 3 (color online). (a) Temperature dependence of the resistivity for $U/t_{\parallel} = 1.5$ and $t_{\perp 1}/t_{\parallel} = 0.1$, with fixed $t_{\perp 2}/t_{\parallel} = 0$, 0.02. 0.04, 0.06, 0.08, 0.10 (from top to bottom), and $\rho_0 = \rho(\Lambda)$. T_ρ is the characteristic temperature of the Mott insulator, at which the resistivity takes a minimum. T_{FL} is the crossover temperature to the metallic Fermi liquid, where the power of $\rho(T)$ exhibits a change (guided by the eyes). (b) Schematic illustration of the $t_{\perp 2}$-T phase diagram. T_{FL}^0 is the bare temperature scale for imperfect nesting [left of Eq. (4)], which is reduced to T_{FL} due to the correlation effects.

neither the FL state nor the crossover region appears in the phase diagram.

We would like to discuss here the impact of our results on the understanding of the phase diagram of the quasi-1D molecular compound (TTM-TTP)I_3 under pressure [5]. The extended Hückel calculations [18] indicate that there are two kinds of interchain transfer integrals, namely $t_{\perp 1} \approx 9$ meV, and $t_{\perp 2} \approx 6$ meV, which are small compared to $t_{\parallel} \approx 260$ meV. This emphasizes the pronounced hopping frustration of this quasi-1D compound. The Coulomb repulsion between electrons on the same molecular orbital of TTM-TTP is weak, and the estimated magnitude, $U \approx 0.57$ eV [3], leads to the magnitude $U/t_{\parallel} \approx 2.2$ and then the small 1D Mott gap $\Delta_\rho^{\mathrm{1D}}/t_{\parallel} \approx 0.24$. From these figures, the energy scale for imperfect nesting [left-hand side of Eq. (4)] turns out to be about 5 meV. As for the magnitude of the charge gap at ambient pressure, we obtain $\Delta_\rho^{\mathrm{1D}} \approx 60$ meV, in fair agreement with the measured activation energy of resistivity at ambient pressure [3]. The bandwidth goes up under pressure, which decreases the ratio $U/t_{\parallel}$ and in turn the charge gap. To reduce the gap down to the scale of imperfect nesting, one has roughly to double the hopping amplitudes. This represents a reasonable increase of band parameters under 8 GPa of pressure, and is consistent with the existence of a MI transition in (TTM-TTP)I_3 [5]. Finally, we note that at ambient pressure, below $T_c \simeq 120$ K, this compound develops a nonmagnetic state (likely of the spin-Peierls type), which comes with an *intramolecular* charge disproportionation [4]. However, since the resistivity already shows an insulating behavior above T_c, the present system can be indeed considered as a Mott insulator rather than a charge-ordered insulator, and the charge disproportionation can be accounted for by dimerization of the tilted TTM-TTP molecules.

In summary, we have examined the effect of interchain frustration on the half-filled quasi-1D Hubbard chains by applying an $N_\perp$-chain two-loop RG method. The triangular lattice geometry of the system is found to be a key factor in the stability of the Mott insulating state and whenever the alteration of nesting conditions due to frustration in the transverse hoppings reaches some threshold a metallic state is restored. Our results find direct application to the description of the frustrated quasi-1D half-filled compounds.

One of the authors (M. T.) thanks S. Yasuzuka, T. Kawamoto, T. Mori, A. Läuchli, T. Giamarchi, and C. Berthod for valuable discussions. This work was supported in part by a Grant-in-Aid for Scientific Research on Priority Areas of Molecular Conductors (No. 15073213) from the Ministry of Education, Science, Sports, and Culture, Japan.

[1] M. Imada, A. Fujimori, and Y. Tokura, Rev. Mod. Phys. **70**, 1039 (1998).
[2] B. J. Kim *et al.*, Nature Phys. **2**, 397 (2006).
[3] T. Mori *et al.*, Phys. Rev. Lett. **79**, 1702 (1997).
[4] T. Mori, Chem. Rev. **104**, 4947 (2004).
[5] S. Yasuzuka *et al.*, J. Phys. Soc. Jpn. **75**, 053701 (2006); J. Low Temp. Phys. **142**, 197 (2006).
[6] I. E. Dzyaloshinskii and A. I. Larkin, Sov. Phys. JETP **34**, 422 (1972).
[7] C. Bourbonnais, B. Guay, and R. Wortis, in *Theoretical Methods for Strongly Correlated Electrons*, edited by D. Sénéchal, A. M. Tremblay, and C. Bourbonnais (Springer, New York, 2003), p. 77.
[8] T. Giamarchi, *Quantum Physics in One Dimension* (Oxford University Press, New York, 2004).
[9] F. H. L. Essler and A. M. Tsvelik, Phys. Rev. B **65**, 115117 (2002).
[10] S. Biermann *et al.*, Phys. Rev. Lett. **87**, 276405 (2001); T. Giamarchi *et al.*, J. Phys. IV (France) **114**, 23 (2004); C. Berthod *et al.*, Phys. Rev. Lett. **97**, 136401 (2006).
[11] M. Tsuchiizu, Phys. Rev. B **74**, 155109 (2006).
[12] M. Tsuchiizu, Y. Suzumura, and C. Bourbonnais, J. Phys. Condens. Matter **19**, 145 228 (2007).
[13] R. Duprat and C. Bourbonnais, Eur. Phys. J. B **21**, 219 (2001); C. Bourbonnais and R. Duprat, J. Phys. IV (France) **114**, 3 (2004).
[14] S. Dusuel and B. Douçot, Phys. Rev. B **67**, 205111 (2003).
[15] D. Rohe and A. Georges, arXiv:cond-mat/0608032.
[16] T. Kashima and M. Imada, J. Phys. Soc. Jpn. **70**, 3052 (2001); B. Kyung and A.-M. S. Tremblay, Phys. Rev. Lett. **97**, 046402 (2006).
[17] T. Giamarchi, Phys. Rev. B **44**, 2905 (1991).
[18] T. Mori *et al.*, Bull. Chem. Soc. Jpn. **67**, 661 (1994).